ELSEVIER

Journal of Alloys and Compounds 293–295 (1999) 593–600

Journal of ALLOYS AND COMPOUNDS

Electrochemical properties and characteristics of a fluorinated AB_2-alloy

Z.P. Li*, E. Higuchi, B.H. Liu, S. Suda

Department of Environmental & Chemical Engineering, Kogakuin University, Nakano-machi 2665-1, Hachioji-shi, Tokyo 192-0015, Japan

Abstract

A series of fluorination techniques have been developed in this laboratory to improve the surface condition of AB_2 alloy. The fluorination was found effective for removing oxide layer and implanting catalytic Ni to the alloy surfaces. The developed fluorination techniques improved considerably the initial activation characteristics, decreased the electrochemical reaction impedance and increased the rate capacity of AB_2 electrodes.

Keywords: Fluorination technique; Specific surface area; Discharge capacity; Rate capacity; Impedance

1. Introduction

AB_2-type alloys, in general, have been found to give a comparatively higher discharge capacity than AB_5-type alloys. However they showed poor activation characteristics and slow kinetic properties because condensed oxides existed on alloy surfaces and low Ni content in the surface layer [1]. It was reported that hot alkaline solution treatment [2] was very effective to improve the electrochemical performances. The constituent element dissolution resulted in forming a Ni-rich layer on alloy surfaces. A chemical plating method has been proposed by Sakai and others [3,4] for the electrical conductivity improvement.

Considering element dissolution and Ni plating, we developed a series of fluorination techniques aiming at building up an active surface layer. The treatment mechanism is proposed to explain the improvement on electrochemical properties of AB_2 alloy by fluorination in this paper.

An aqueous fluorine-containing solution (denoted by F-solution) has been applied for treating the surface of AB_2 alloy particles [5,6]. The conventional fluorination technique was found effective in eliminating oxide layer from surfaces of AB_2 alloys where the Zr and Mn dissolved easily into the F-solution by forming complex ions. An F-solution containing NiF_2, reductant (sodium phosphinate monohydrate) and ligand (trisodium citrate dihydrate) for stabilizing Ni^{2+} was developed in order to coat metallic Ni in the surface layer.

Furthermore, we applied active metal elements on alloy surfaces to implant metallic Ni clusters distributing homogeneously in the surface layer. It was found that this new method showed significant effects on improving the discharge properties of AB_2 alloys. More advanced fluori-

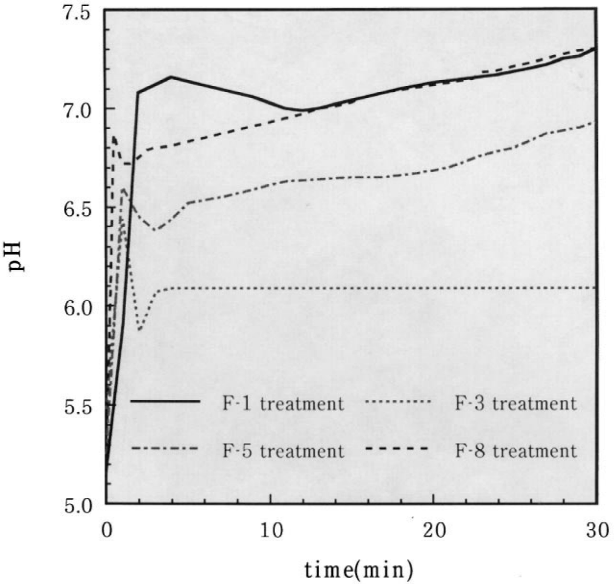

Alloy : $Zr_{0.9}Ti_{0.1}V_{0.2}Mn_{0.6}Co_{0.1}Ni_{1.1}$
Powder : 10 times hydriding-dehydriding cycling
Podwer size : 15.5 μm
treatment temperature : 70℃
treatment condition : 0.05g alloy/ml solution

Fig. 1. The pH change during fluorination treatment.

---

*Corresponding author.

0925-8388/99/$ – see front matter
PII: S0925-8388(99)00415-6

nation techniques combined with ball milling have been found effective on improving rate capacity and decreasing reaction impedance of AB_2 electrode.

2. Experimental details

A typical AB_2-type alloy, $Zr_{0.9}Ti_{0.1}V_{0.2}Mn_{0.6}Co_{0.1}Ni_{1.1}$ has been chosen as the test alloy. The alloy was prepared from pure metals by induction melting. Ingots were annealed for 18 h at 1100°C under Ar atmosphere. The alloy was pulverized by 10 hydriding–dehydriding cycles before fluorination. The powder average size was 15.5 μm with specific surface area of 0.228 m^2/g. The hydride electrodes were made by mixing alloy powder with PTFE powder in a weight ratio of 20:1, packing by Ni-grid of 100 mesh then pressing into pellets with diameter of 13 mm and thickness about 1.5 mm under a mechanical load of 4 ton/cm^2. The electrodes were cycled by charging at current of 34 mA/g for 13 h then discharging at current of 68 mA/g to cut-off voltage of −0.6 V vs. Hg/HgO electrode in 6N KOH after resting 1 h at 20°C. The rate capacity was measured after activation.

3. Results and discussion

3.1. Fluorination techniques

3.1.1. F-1 treatment

One litre of treatment solution (F-1 solution) was made from 6 g KF and 0.6 ml HF aqueous solution. During the fluorination treatment by the F-1 solution at 70°C (so called F-1 treatment), the pH-value changes from pH=5.3 up to 7.3 as shown in Fig. 1. The pH change was caused by the removal of oxide layer on the surface and the dissolution of metallic elements (mostly Zr and Mn) into the solution through the following reactions:

$$ZrO_2 + 6F^- + 2H_2O = [ZrF_6]^{2-} + 4OH^- \quad (1)$$

$$Zr + Mn + 12F^- + 6H_2O = [ZrF_6]^{2-} + [MnF_6]^{4-} + 6H + 6OH^- \quad (2)$$

The metallograph of the treated ingot specimen is shown in Fig. 2(b). Fig. 3(a) shows the element dissolution after F-1 treatment at 70°C for 30 min. The dissolution of Zr and Mn was reconfirmed by EPMA as shown in Fig. 4.

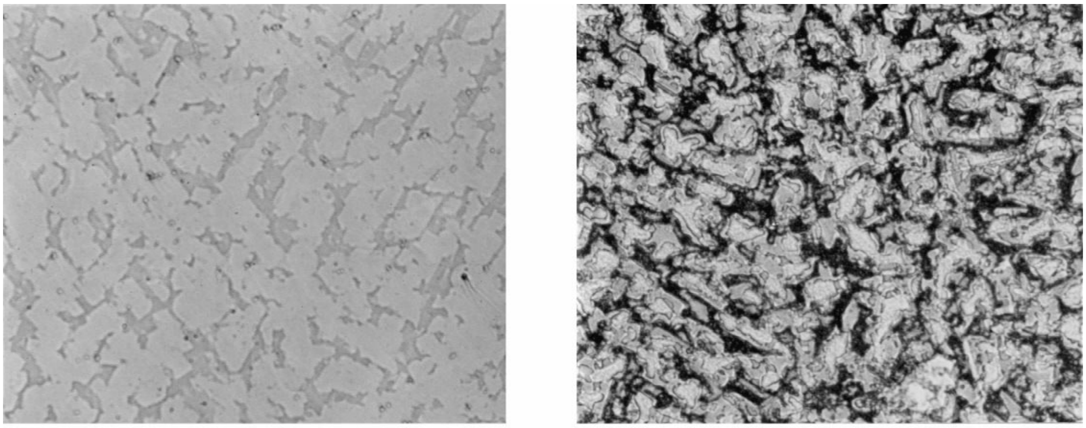

(a)Original (b)F-1 treated

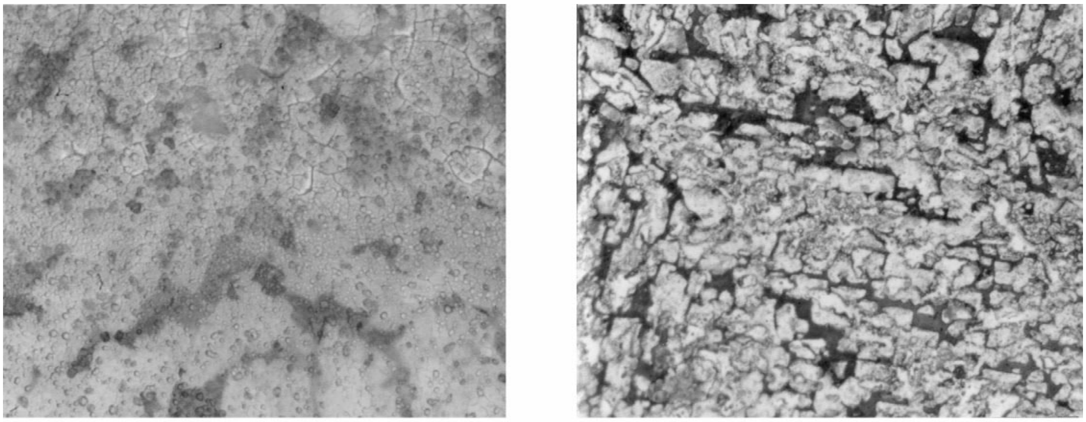

(c)F-3 treated (d)F-5 treated

Fig. 2. The metallographic pictures of treated ingot specimen of AB_2 alloy at 70°C.

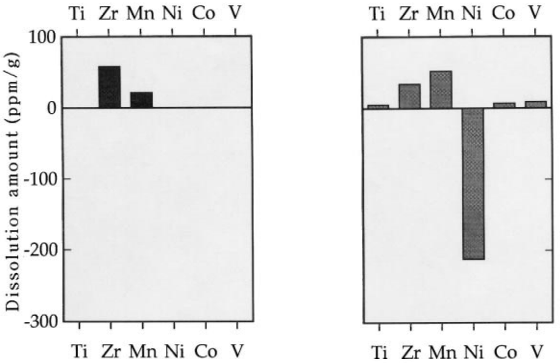

(a) F-1 treatment (b) F-3 treatment

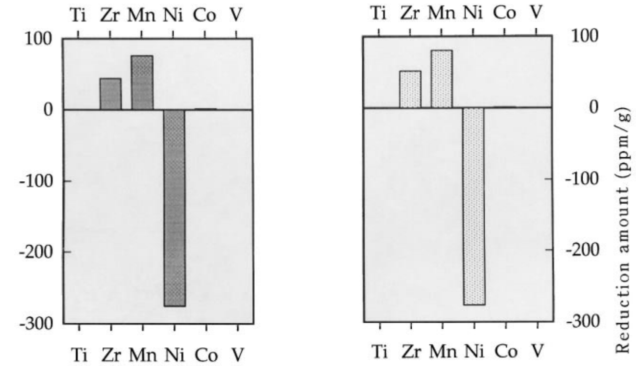

(c) F-5 treatment (d) F-8 treatment

Fig. 3. The element dissolution and reduction behaviour of Zr-based AB_2 alloy after each fluorination treatment.

3.1.2. F-3 treatment

Based on F-1 solution, another F-solution (F-3 treatment solution) contains NiF_2 and reductant such as sodium phosphinate monohydrate was prepared for coating metallic Ni on the alloy surfaces. A ligand such as trisodium citrate dihydrate was added to stabilize Ni^{2+} ions by preventing the precipitation of metallic Ni out of alloy surfaces. It was believed that the Ni precipitated through the following reaction, similar to Ni chemical plating process [7].

$$2H_2PO_2^- + 2H_2O + [Ni^{2+}C_6H_5O_7^{3-}] = Ni^0 + 2HPO_3^{2-} + 4H^+ + H_2 + C_6H_5O_7^{3-} \quad (3)$$

where $C_6H_5O_7^{3-}$ is the ligand, and $H_2PO_2^-$ is the reductant.

Because of the oxide elimination capability of F^- ions, it did not need any pretreatment procedure to coat Ni. The pH-value increased firstly from $pH=5.3$ up to 6.4 then decreased to 6.1 during treatment (shown in Fig. 1). Since then, the pH-value kept constant. The increase of pH-value was due to the reactions for the removal of oxide layer and the dissolution of metallic elements through reaction (1) and (2). Decrease of pH-value was caused by the Ni reduction reaction (3). The metallic Ni clusters would grow on metallic surfaces (mainly metallic Ni). The metallograph of the treated ingot specimen is shown in Fig. 2(c). Fig. 3(b) shows the element dissolution and Ni reduction after F-3 treatment at 70°C for 30 min.

3.1.3. F-5 treatment

In order to improve the metallic Ni distribution on alloy surfaces, the constituent metallic Zr and Mn on alloy surfaces were used as the reductant to implant metallic Ni on the surfaces. Ni can be implanted on the spots where Zr and Mn were dissolved into the treatment solution and left through following reaction:

$$Zr + Mn + 3[NiF_6]^{4-} = [ZrF_6]^{2-} + [MnF_6]^{4-} + 3Ni + 6F^- \quad (4)$$

The pH change during treatment is shown in Fig. 1. The increase of pH-value is caused by oxide removal by reaction (1). The low pH-value compared with F-1 treatment, can be attributed to the reaction (4) because one part of Zr and Mn dissolution has no contribution to the pH increase. By changing treatment solution, it is possible to control the morphology and fine structure of Ni-rich layer formed on the surfaces. The Zr, Mn dissolution and Ni reduction have been confirmed by metallurgical observation and ICPs analyses for the $Zr_{0.9}Ti_{0.1}V_{0.2}Mn_{0.6}Co_{0.1}Ni_{1.1}$ alloy (shown in Fig. 2(d) and Fig. 3(c)).

3.1.4. F-8 treatment

Among these treatment methods mentioned above, the alloy was pulverized by hydriding–dehydriding cycling. The average size of the particles was around 15 μm through 10 hydriding–dehydriding cycles. It was not enough to obtain higher rate capacity and lower reaction impedance so that we applied wet ball milling to pulverize the alloy to get much smaller particles before F-5 treatment. The pH change during F-8 treatment is similar to the F-5 treatment as shown in Fig. 1. It was believed that the treatment mechanism was similar to the F-5 treatment.

3.1.5. F-9 treatment

To modify the original passive surfaces of AB_2 alloy, we developed a much simpler method combining fluorination and pulverization together. The alloy was treated by mixing alloy powders, NiF_2 with F-1 solution through planetary ball mill. The starting size of the alloy before grinding was smaller than 75 μm. The alloy was pulverized and fluorinated during ball milling at room temperature. It is believed that the fluorination mechanism is similar to the F-5 treatment.

3.2. Structure, P–c–T, surface and specific surface area

3.2.1. XRD analysis and P–C–T property

By XRD analysis, it was found the structure of all the treated alloys kept unchanged as shown in Fig. 5. The *P–C–T* property changed as shown in Fig. 6. It implied

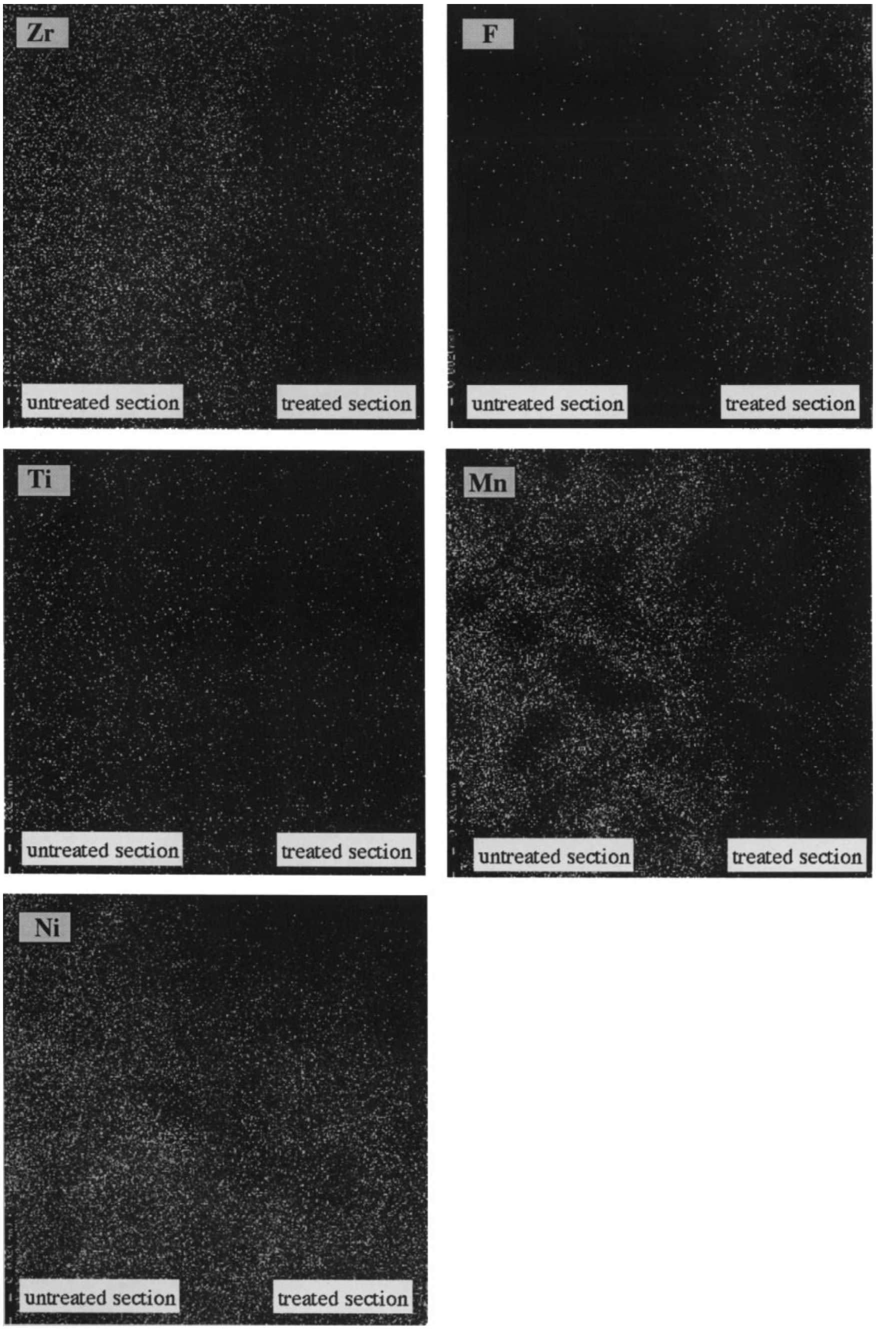

Fig. 4. The comparison of the element distribution after F-1 treatment of Zr-based AB_2 alloy.

that all the treatments only modified the alloy surface. The improvement of electrochemical performances was brought by the surface modification.

3.2.2. Surface and specific surface area

The untreated surface can be modified through fluorination. F-1 treatment removed the oxide layer and Zr, Mn dissolved to treatment solution, which increased the specific surface area a little.

Metallic Ni was implanted on alloy surfaces by F-3 treatment, meanwhile Zr and Mn dissolved to the treatment solution. The plated Ni formed a consistent Ni layer on alloy surfaces because Ni grew on the metallic Ni as shown in Fig. 7(a).

For the F-5 treatment, metallic Ni was implanted on the spots where Zr or Mn dissolved. That means, the growth of Ni layer depends on the Zr and Mn dissolution. Contrary to F-3 treatment, Ni could not deposit on the metallic Ni. Combined with the constituent Ni on alloy surfaces, F-5 treatment can produce a well-dispersed Ni network on

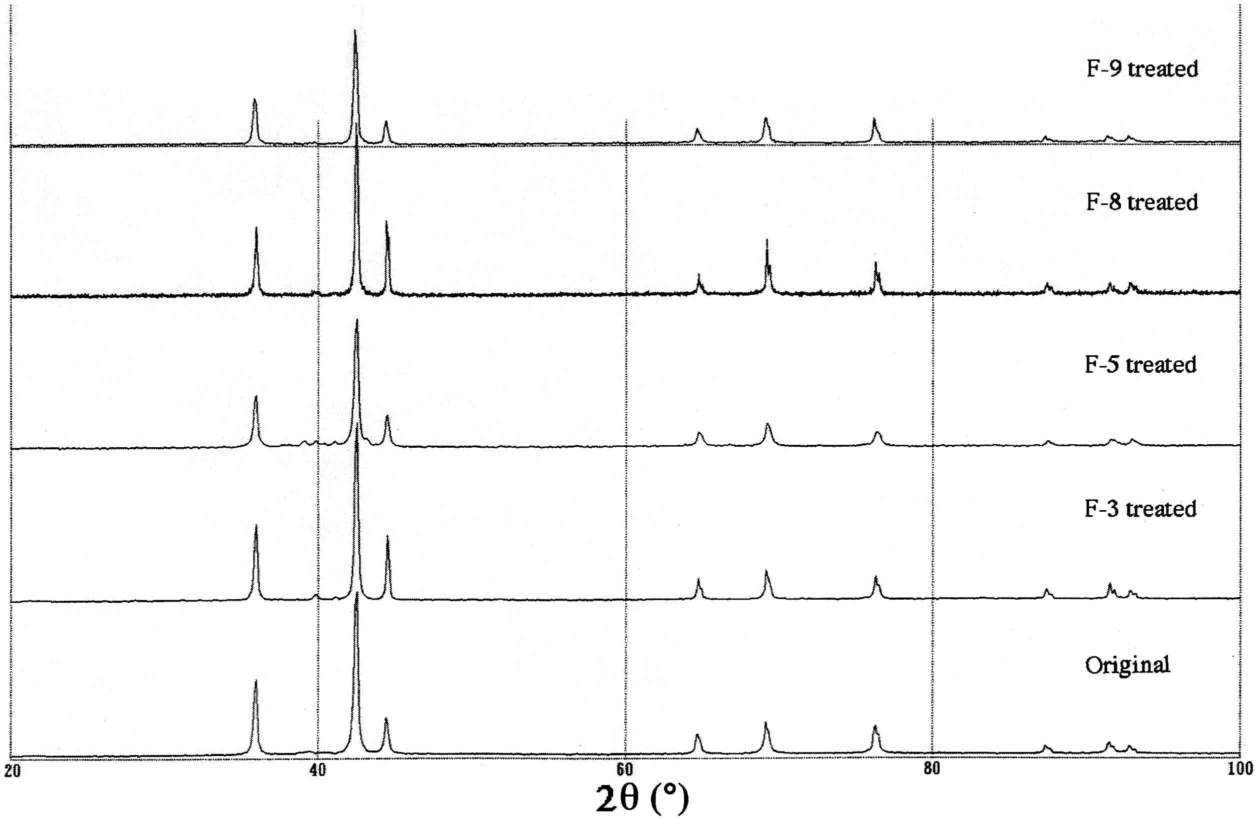

Fig. 5. The XRD pattern of fluorinated AB_2 alloys.

alloy surfaces comparing with F-3 treatment. Fig. 7(b) shows the surface structure of fluorinated alloy powders by F-5 treatment.

Fig. 8 shows the increase of specific surface area through each treatments. F-8 and F-9 treatment increased specific surface areas greatly so that the specific electrochemical catalysis of the alloy improved dramatically after fluorination. The SEM results showed the fine surface structures of fluorinated AB_2 alloy in Fig. 7(c,d).

3.3. Electrochemical characteristics and properties

3.3.1. Electrochemical activation and rate capacity

From Figs. 9,10, we can see that fluorination can increase the initial and maximum discharge capacity of the AB_2-type alloy. Through F-treatments, the oxides were taken away by F-ions to form soluble complex ions, meanwhile the metallic Ni deposited on the surfaces so that the activation and rate discharge properties were improved. The rate capacities of fluorinated AB_2 alloy increased in accordance with the Ni reduction (Fig. 3) and specific surface area increase (Fig. 8) as shown in Fig. 11. It was believed that the rate capacity and activation property were improved due to the increase of catalytic site in unit surface area through fluorination treatment.

3.3.2. Electrochemical kinetics and impedance

As an example, Fig. 12 shows the cyclic voltammetry of F-5 treated AB_2 electrode. Its steady state I/E analysis and impedance analysis showed that fluorination treatment improved the initial charge property, increased the exchange current density and decreased the electrochemical reaction impedance (Figs. 13, 14). It can be attributed to the well-dispersed Ni network formed on alloy surfaces by fluorination as shown in Fig. 7.

4. Conclusions

During fluorination treatments of the AB_2 alloy, Zr and Mn dissolved from alloy surfaces meanwhile metallic Ni was implanted to the alloy surfaces. The specific surface area increased through surface modification by fluorination treatment.

Fluorination treatment can decrease the reaction impedance and improve the surface catalysis to increase the

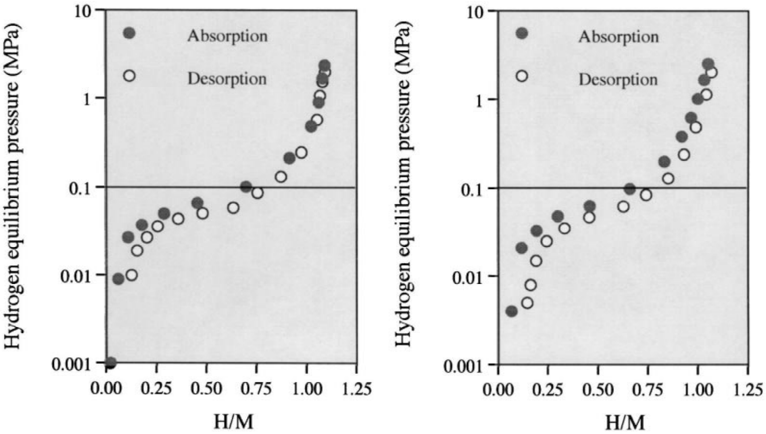

Untreated

F-1 treated

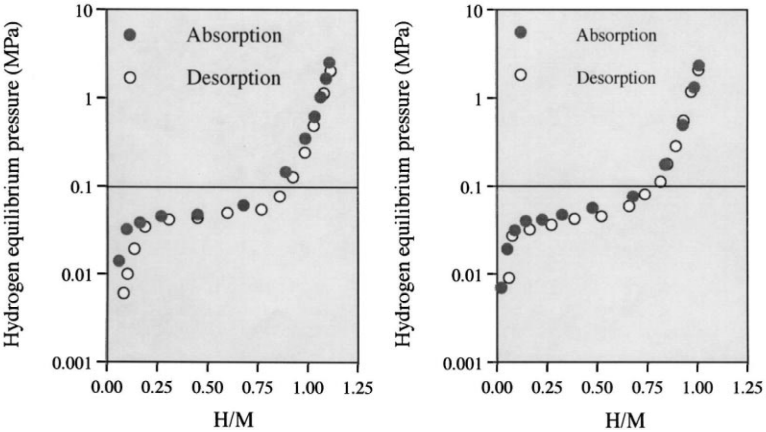

F-3 treated

F-5 treated

Fig. 6. P–C–T property of fluorinated AB_2 alloys at 40°C.

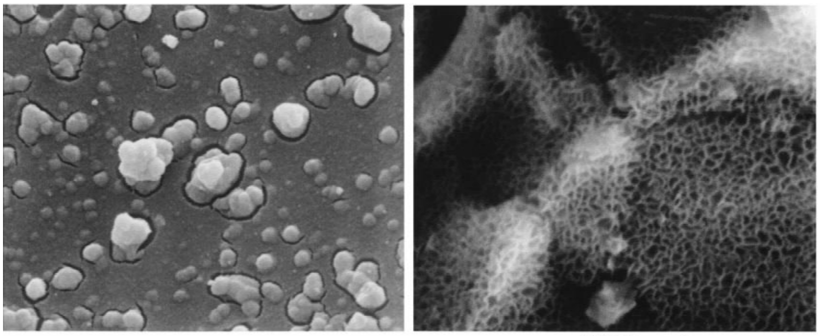

(a)F-3 treated

(b)F-5 treated

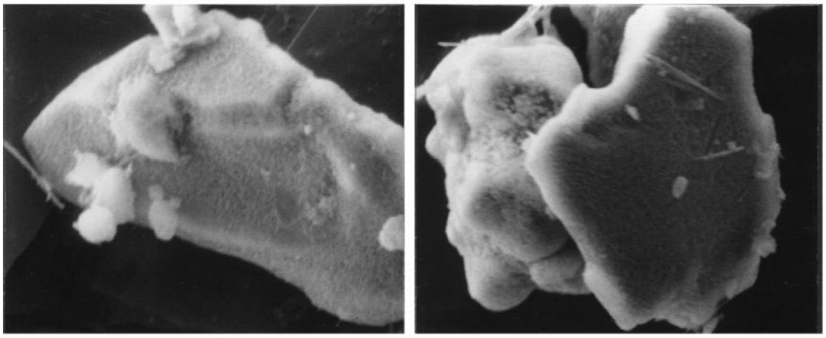

(c)F-8 treated

(d)F-9 treated

Fig. 7. The fine structures of fluorinated AB_2 alloy surface.

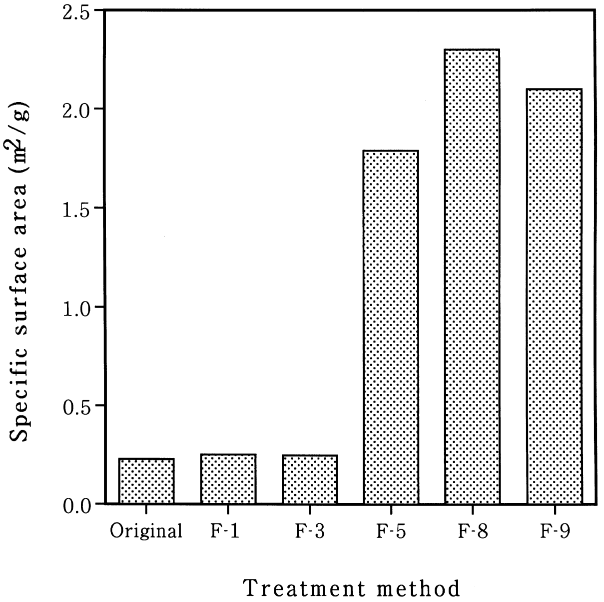

Fig. 8. The specific surface area of fluorinated AB_2 alloys.

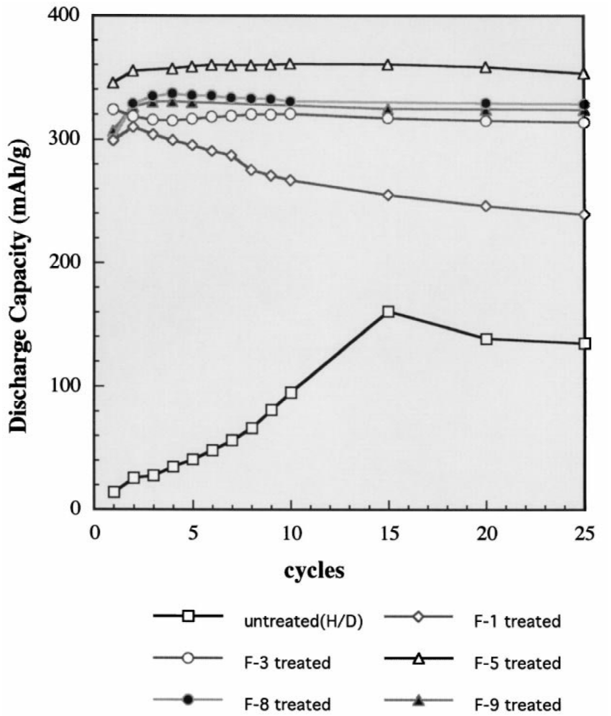

Alloy:	$Zr_{0.9}Ti_{0.1}V_{0.2}Mn_{0.6}Co_{0.1}Ni_{1.1}$
Pellet size:	Φ13mm; thickness: 1.5mm
Pellet composition:	alloy/PTFE=5/1
Alloy weight:	1.0g
Charge current:	34mA/g for 13h
Discharge current:	68mA/g to -0.6V vs. Hg/HgO 6N KOH
Temperature:	20°C

Fig. 9. The activation property of fluorinated AB_2 alloys.

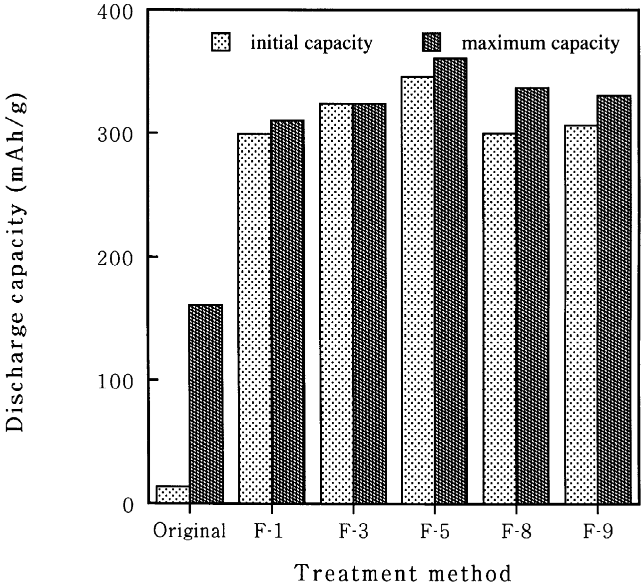

Fig. 10. The initial discharge capacity and maximum capacity of fluorinated AB_2 alloys.

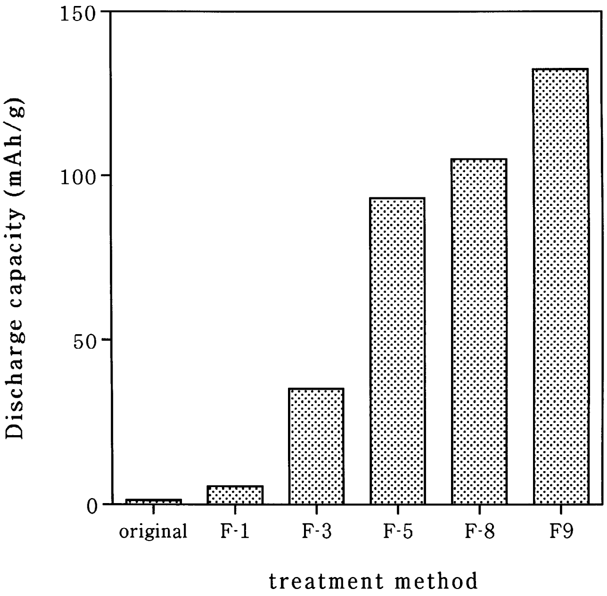

Fig. 11. The rate discharge capacity of fluorinated AB_2 alloy. Discharge current: 1.5 C = 520 mA/g.

exchange current density so that the electrochemical activation and rate discharge capacity were improved.

Acknowledgements

This work has been supported by the New Energy Development Organization. We are thankful to Mr. A. Okutsu and H. Ohta for their efforts on the research.

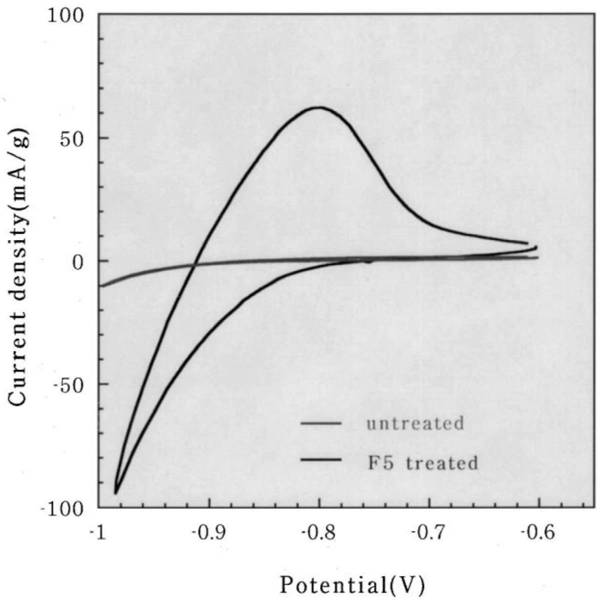

Fig. 12. The CV curve of F-5 treated $Zr_{0.9}Ti_{0.1}V_{0.2}Mn_{0.6}Co_{0.1}Ni_{1.1}$ alloy. Alloy: 10 times hydriding–dehydriding cycled. Electrode: before charging–discharging cycling. Temperature: 20°C. Scan speed: 0.5 mV/s.

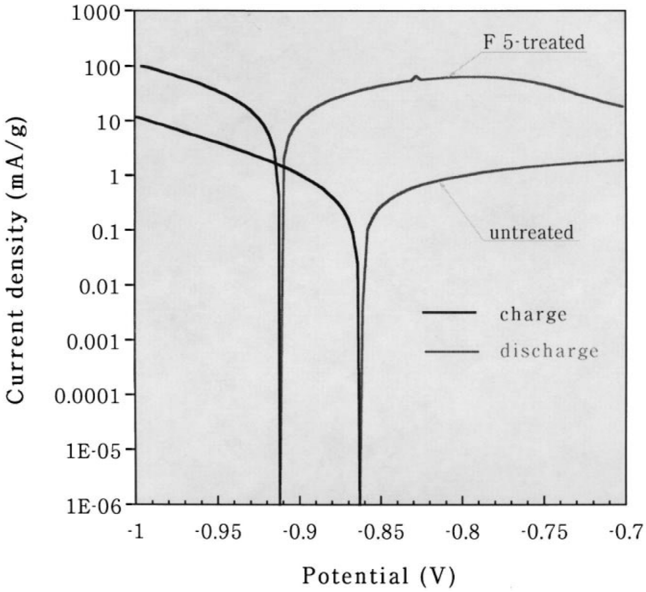

Fig. 13. The IE curve of F-5 treated $Zr_{0.9}Ti_{0.1}V_{0.2}Mn_{0.6}Co_{0.1}Ni_{1.1}$ alloy. Alloy: 10 times hydriding–dehydriding cycled. Electrode: before charging–discharging cycling. Temperature: 20°C.

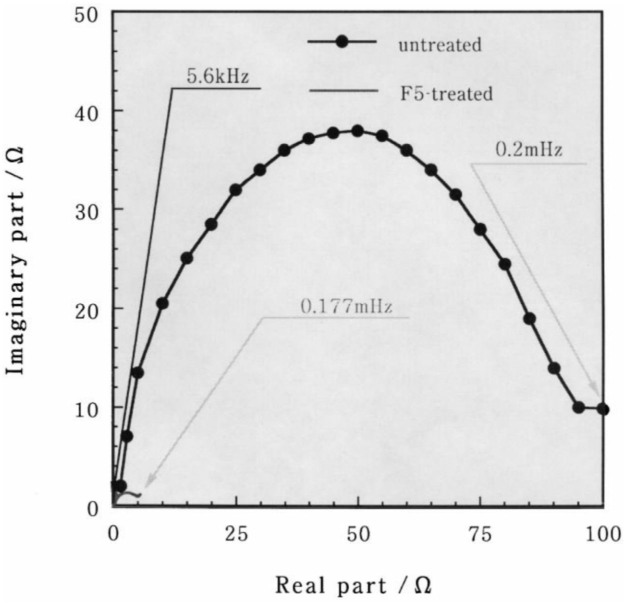

Fig. 14. The impedance of F-5 treated $Zr_{0.9}Ti_{0.1}V_{0.2}Mn_{0.6}Co_{0.1}Ni_{1.1}$ alloy. Alloy: 10 times hydriding–dehydriding cycled. Electrode: before charging–discharging cycling. Temperature: 20°C.

References

[1] H. Sawa, M. Ohta, H. Nakano, S. Wakao, Z. fur Phy. Chem. N.F. 164 (1989) 1527.
[2] B.K. Zoitos, D.L. Hudson, P.D. Bennett, V.J. Puglisi, Electrochem. Soc. Proc. 92 (5) (1992) 168.
[3] T. Sakai, H. Ishikawa, K. Oguro, C. Iwakura, Prog. Batteries Sol. Cells 6 (1987) 221.
[4] T. Sakai, H. Ishikawa, K. Oguro, C. Iwakura, H. Yoneyama, J. Electrochem. Soc. 134 (3) (1987) 558.
[5] S. Suda, Jpn. Tokkyo, No: 4-199231, (1992).
[6] S. Suda, Jpn. Tokkyo, No: 8-118098, (1996).
[7] R.M. Lukes, Plating 51 (1964) 969.